JOURNAL OF MATERIALS SCIENCE 22 (1987) 3517–3521

Electrochemical polarization and pitting behaviour of Fe–Al–Mn alloys in chloride solutions

WEN-TA TSAI, JING-BANG DUH, JU-TUNG LEE
Department of Metallurgy and Materials Engineering, National Cheng Kung University, Tainan, Taiwan

The electrochemical polarization behaviour of the austenitic Fe–8.25 Al–29.95 Mn–0.85 C and Fe–9.33 Al–25.94 Mn–1.45 C alloys, either solution-annealed and/or age-treated, was investigated in 3.5 wt% NaCl solution. Potentiodynamic polarization tests showed that these alloys passivated with difficulty and had much higher anodic passive current densities than that of the conventional austenitic 316 stainless steel (SS). The susceptibility to pitting corrosion of these alloys under open-circuit potential conditions was also studied in 6% $FeCl_3$ solution. Metallographical examination indicated that pitting and general corrosion occurred on the specimen surfaces. The corrosion rates of these alloys were about one order of magnitude higher than that of the AISI 316 SS. In general, the corrosion resistances of the Fe–Al–Mn alloys studied were inferior to that of the conventional stainless steel.

1. Introduction

Conventional Fe–Cr–Ni alloys have been widely and successfully used in industry for many years because of their good corrosion resistance and mechanical properties. On the basis of economic and strategic considerations, however, there are demands to develop new alloys to substitute for these conventional stainless steels (SS). Among the most promising alloys which could serve as effective candidates are the Fe–Al–Mn alloys. The Fe–Al–Mn alloys have many advantages, for example lower cost, low density, excellent mechanical strength and good oxidation resistance [1, 2]. Thus, the development of Fe–Al–Mn alloys has attracted considerable attention from researchers in the past few years.

Although the Fe–Al–Mn alloys have been reported to exhibit good high-temperature oxidation resistance [3–5], very little information concerning the corrosion behaviour of these alloys in aqueous environments is available in the literature. In recent work by Wang and Rapp [6], the electrochemical behaviour of several ferritic Fe–Al–Mn alloys of varying compositions were investigated in 1 N H_2SO_4 or in artificial sea-water. They found that ferritic Fe–Al–Mn alloys, with respective aluminium and manganese contents less than 10 and 8 wt%, had better electrochemical properties than Fe–10 Cr alloy in both 1 N H_2SO_4 solution and artificial sea-water. They pointed out that aluminium could provide passivity for these materials in sulphuric acid solution. However, alloys with aluminium content less than 10 wt% were not adequate for marine application as far as corrosion resistance was concerned. The adverse effect of manganese was also recognized by noting the raise of the primary passive potential and the critical current density in sulphuric acid.

The corrosion resistances in sea-water of the austenitic Fe–Al–Mn alloys, which contain more manganese, were investigated by Wang and Beck [2]. They claimed that these austenitic alloys were not susceptible to stress-corrosion cracking in sea water. Moreover, based upon the electrochemical polarization data, they found that the corrosion rate of Fe–10 Al–30 Mn–C–Si alloy in sea water was lower than that of 18 Cr–9 Ni–Ti stainless steel. Although corrosion resistance may be derived from aluminium, it is still surprising and unexpected to see that the Fe–Al–Mn alloys exhibited better corrosion resistance than AISI 321 SS. In this study, the electrochemical properties and pitting behaviour of three austenitic Fe–Al–Mn alloys in chloride solutions were, thus, investigated and their corrosion resistances were further evaluated.

2. Experimental procedure

Two alloys of compositions Fe–8.25 Al–29.95 Mn–0.85 C and Fe–9.33 Al–25.94 Mn–1.45 C were prepared by melting pure iron, aluminium and manganeses in a laboratory induction furnace under an argon protective atmosphere, and were then cast into a steel mould. The cast ingots were hot-forged into 11 mm thick billets at 1250° C. These billets were homogenized at 1100° C for 8 h, oil-quenched and then cold-rolled to 3 mm. These materials were subsequently solution-annealed at 950° C for 1 h and then oil-quenched. Specimens which were machined from the materials with compositions of Fe–8.25 Al–29.95 Mn–0.85 C and Fe–9.33 Al–25.94 Mn–1.45 C were designated as A and C, respectively. Specimen B was the designation for material containing 0.85 wt % C which was age-treated (AT) at 550° C for 4 h after solution-annealing. For comparison, AISI 316 SS

0022–2461/87 $03.00 + .12

with solid-solution treatment at 1100° C for 1.5 h was also used (Specimen D).

Electrochemical polarization curves were obtained using a potentiodynamic technique. Samples with about 120 mm^2 exposed surface area were connected with copper wires that were covered with heat-shrinkable Teflon tubes, and mounted on to epoxy resin. They were then ground by 600 grit silicon carbide paper, washed in distilled water and rinsed in acetone prior to use. To avoid interference from crevice corrosion, the mounted electrodes were painted at the resin–alloy interface with an alkyd varnish. The tests were then conducted in a glass cell in which a solution containing 3.5% NaCl with a pH of 6.0 was de-aerated by purging with nitrogen. Before a test the electrodes were cathodically polarized at a potential approximately 200 mV more negative than the open-circuit potential. Potentiodynamic polarization curves were obtained at a potential scan rate of 60 mV min^{-1}. All potentials were measured with respect to a saturated calomel electrode (SCE). After the polarization test, each specimen was examined under an optical microscope and scanning electron microscope (SEM).

Pitting corrosion tests under open-circuit potential conditions were also conducted in 6% $FeCl_3$ solution at 25° C. Rectangular coupons with dimensions of 2 mm × 10 mm × 10 mm were used. Each specimen was polished to a 1000 grit silicon carbide finish, degreased in acetone in an ultrasonic cleaner, and finally washed in distilled water and dried in air. A cradle made of glass was used to hold the specimen. The specimen contained in the cradle was placed inside a 100 ml beaker and completely immersed in the test solution. The weight loss of each specimen after a 3-day test was measured and the corrosion rate was calculated accordingly. The surface morphology of each specimen after the immersion test was examined under the SEM. Energy-dispersive spectrometry (EDS) was also used to analyse the corrosion product formed on the specimen surface.

3. Results and discussion

Potentiodynamic polarization curves for the three Fe–Al–Mn alloys and AISI 316 SS in 3.5% NaCl solution are given in Fig. 1. For Type 316 SS (Curve D in Fig. 1) the corrosion and the pitting potentials were −420 and +280 mV (SCE), respectively. In 3.5% NaCl solution, the conventional austenitic stainless steel exhibited a broad passive range with a passive current density of about 5×10^{-2} A m^{-2}.

For Fe–Al–Mn alloys containing 0.85 wt % C (Curve A in Fig. 1) and 1.45 wt % C (Curve C in Fig. 1), both in the solid-solution condition, the corrosion potentials were −860 and −840 mV (SCE), respectively. The pitting potentials for these two alloys were all about −500 mV (SCE). From Fig. 1 it was found that the polarization curves for these two alloys were almost the same, except that the one containing 0.85 wt % C had a lower anodic current density. The passive current densities of alloys containing 0.85 and 1.45 wt % C were 5×10^{-1} and 8×10^{-1} A m^{-2}, respectively. A wide anodic peak and a narrow passive region were observed for each Fe–Al–Mn alloy which was solid-solution treated. The electrochemical results revealed in Fig. 1 indicated that these two alloys were not easily passivated in chloride solution. The poor passivation property is probably attributed to the high manganese content in these alloys. This result is similar to that observed in Cr–Ni–Mn stainless steel by Lunarska *et al.* [7], who found that increasing the manganese content in Cr–Ni–Mn stainless steel can cause a decrease of the ability to passivate in chloride solution.

For age-treated Fe–8.25 Al–29.95 Mn–0.85 C alloy, the shape of the polarization curve is similar to that of the solution-annealed one (see Curve B in Fig. 1). The corrosion and pitting potentials of this alloy were −850 and −500 mV (SCE), respectively. A broad active peak and a narrow passive region indicate that this alloy is difficult to passivate in a chloride environment. Like the solution-annealed alloys, the

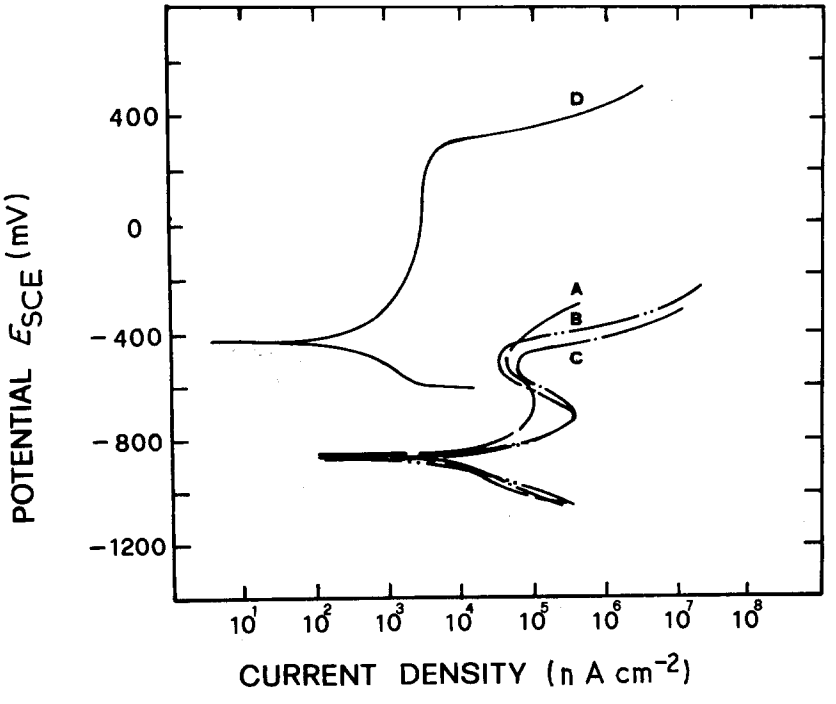

Figure 1 The polarization curves of Fe–Al–Mn Alloys A to C and D (AISI 316 SS) in 3.5% NaCl at 25° C. Scan rate 60 mV min^{-1}.

TABLE I Electrochemical parameters* for AISI 316 SS and Fe–Al–Mn alloys in 3.5% NaCl solution at 25° C

Alloy	E_{corr} (mV_{SCE})	E_{cr} (mV_{SCE})	E_{pp} (mV_{SCE})	i_p ($A\,m^{-2}$)
316 SS	−420	–	280	5.0×10^{-2}
Alloy A	−860	−650	−500	5.0×10^{-1}†
Alloy B	−850	−720	−500	3.0×10^{-1}†
Alloy C	−840	−720	−500	8.0×10^{-1}†

*E_{corr} = corrosion potential, E_{cr} = critical potential for active–passive transition, E_{pp} = pitting potential, i_p = passive current density.
†Minimum current density.

anodic current density in the passive region, 3×10^{-1} A m^{-2}, is approximately one order of magnitude higher than that of AISI 316 SS. Ageing at 550° C for 4 h would cause the precipitation of an Fe_3AlC_x phase in the austenite phase [8]. From the present results, however, it seems that the presence of Fe_3AlC_x precipitate did not affect the electrochemical behaviour of the Fe–Al–Mn alloy in 3.5% NaCl solution. The characteristic electrochemical parameters of the alloys tested in the 3.5% NaCl solution are listed in Table I.

The surface appearance of each specimen was examined after the polarization test. The results for the Fe–Al–Mn alloys are shown in Fig. 2. A large number of pits were formed on the specimen surfaces. Most of these pits were open with a shallow circular shape. Fig. 3 gives an example of the hemispherical pit morphology. The pits formed on Fe–Al–Mn alloys after the polarization test are quite different from those on austenitic stainless steel, which exhibit a deep and concave morphology under the same testing condition (Fig. 4).

Free pitting corrosion tests were conducted in 6% $FeCl_3$ solution (pH 1.2). The corrosion rates for all specimens after a 3-day test are listed in Table II. The respective corrosion rates for Alloys A, B, and C were 138, 121 and 105 mm per year, which were approximately one order of magnitude higher than that for AISI 316 SS (8 mm per year). The results clearly indicate that the corrosion resistances of these three Fe–Al–Mn alloys are inferior to that of AISI 316 SS in $FeCl_3$ solution. The surface appearances of these specimens after immersion tests in 6% $FeCl_3$ are shown in Fig. 5. Although discrete pits were found on the AISI 316 SS specimen surface (Fig. 5a), it was not severely corroded with the grinding scratches still remaining on the surface. Figs 5b to d, however, show that extensive general corrosion as well as pitting corrosion occurred on the Fe–Al–Mn alloy surfaces. Pronounced pitting corrosion was seen for Alloy A (solution-treated Fe–8.25 Al–29.95 Mn–0.85 C). For Alloy C, pitting corrosion was found to a lesser extent compared with Alloy A, and this gave rise to the lower corrosion rate measured. A cross-section of the corroded specimen was also examined after the immersion test. Fig. 6 depicts the rough surface appearance of Alloy B, illustrating the severe attack on the specimen in 6% $FeCl_3$ solution. EDS analysis of the pit bottom gave results consistent with the chemical composition of the Fe–Al–Mn alloy but, in addition, revealed the presence of a small amount of chlorine (Fig. 7).

From the experimental results, it was found that the three austenitic Fe–Al–Mn alloys with the chemical composition given above exhibited very poor corrosion resistance as compared with the conventional 316 SS. The results obtained in this study were not consistent with those found for Fe–10 Al–30 Mn–C–Si alloy [2]. The difference was probably attributable to the fact that the alloy used in the latter case contained 1 wt % Si.

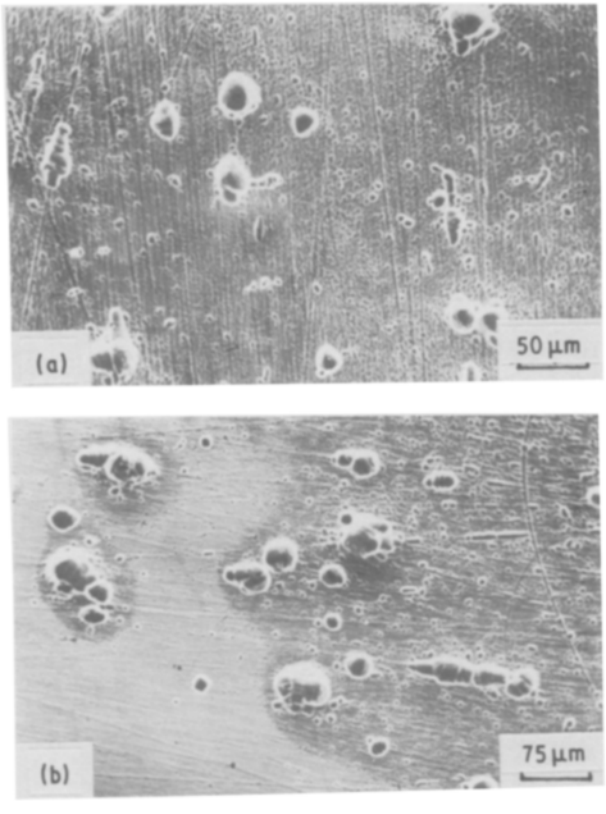

Figure 2 Surface appearance of various alloys after polarization test: (a) Fe–8.25 Al–29.95 Mn–0.85 C, solution-treated (Alloy A), (b) Fe–8.25 Al–29.95 Mn–0.85 C, age-treated (Alloy B), and (c) Fe–9.33 Al–25.94 Mn–1.45 C, solution-treated (Alloy C).

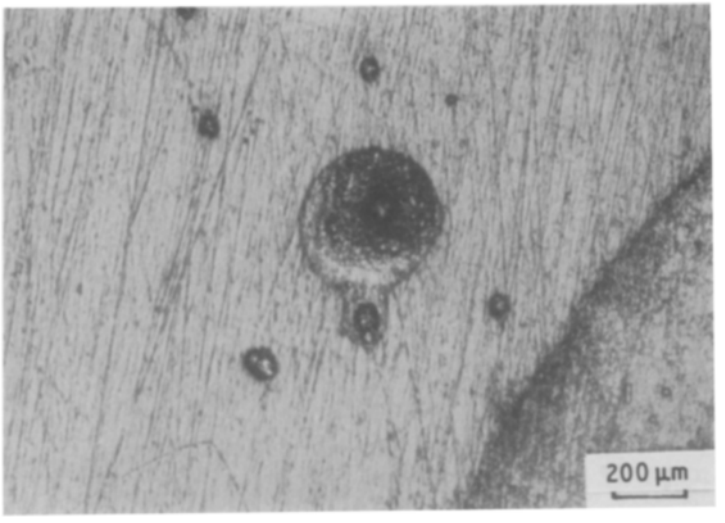

Figure 3 Hemispherical pit formed on the specimen surface of age-treated Fe–8.25 Al–29.95 Mn–0.85 C alloy after potentiodynamic polarization test in 3.5% NaCl at 25° C.

Figure 4 Deep, concave pit formed on solid-solution treated AISI 316 SS specimen surface, after potentiodynamic polarization test in 3.5% NaCl at 25° C.

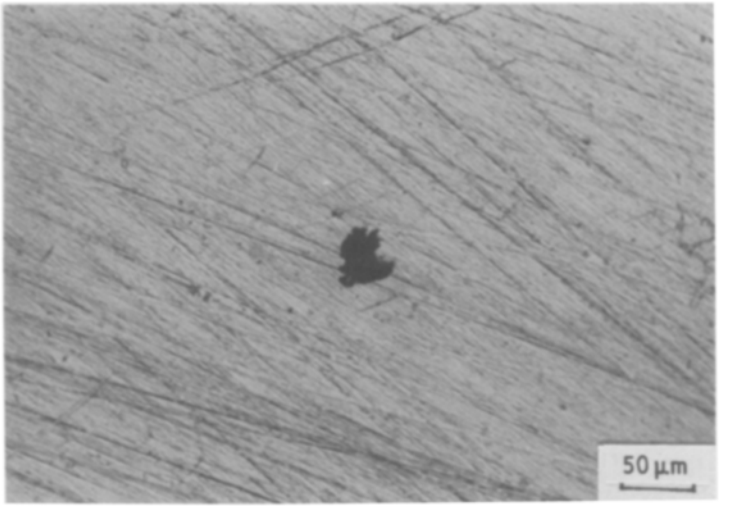

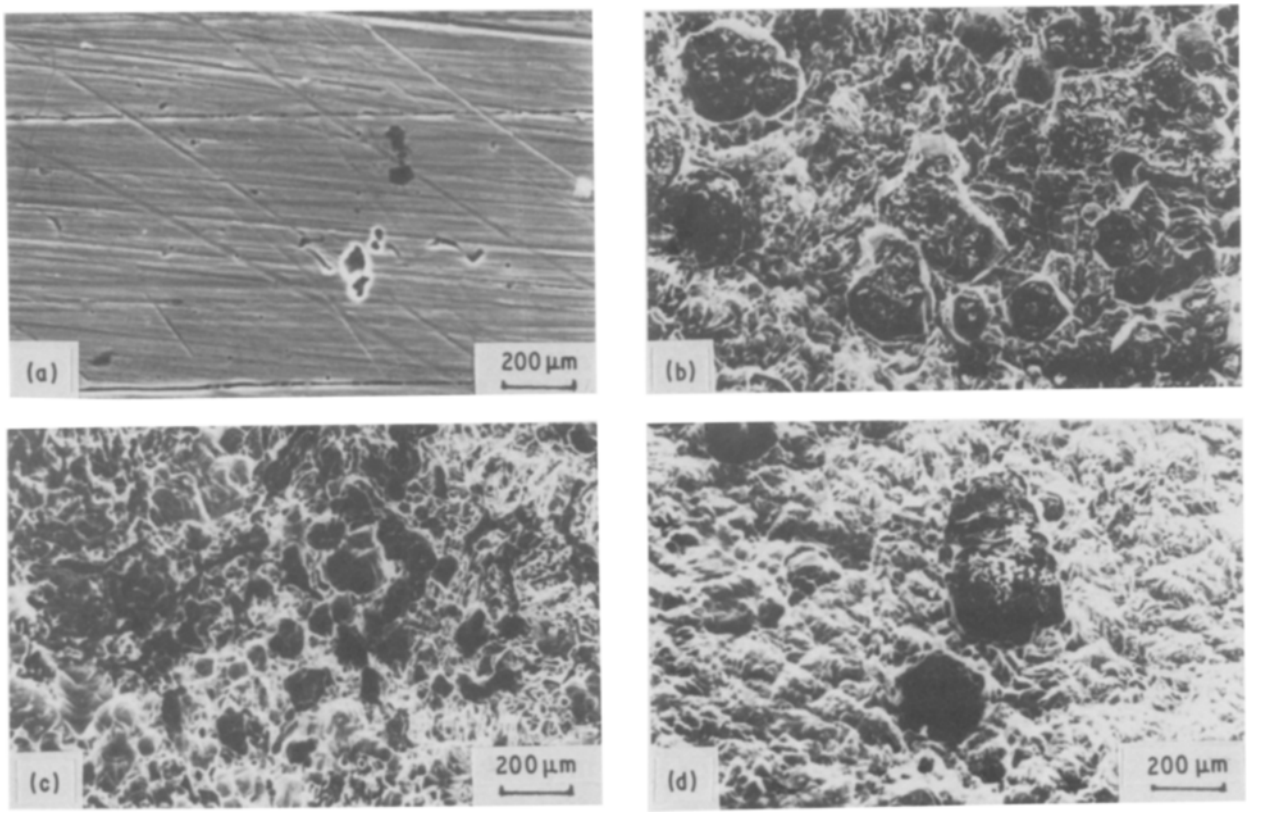

Figure 5 Surface appearance of various alloys after being immersed in 6 wt % $FeCl_3$ at 25° C for 3 days: (a) AISI 316 SS, solution-annealed, (b) Fe–8.25 Al–29.95 Mn–0.85 C, solution-annealed, (c) Fe–8.25 Al–29.95 Mn–0.85 C, age-treated, and (d) Fe–9.33 Al–25.94 Mn–1.45 C, solution-annealed.

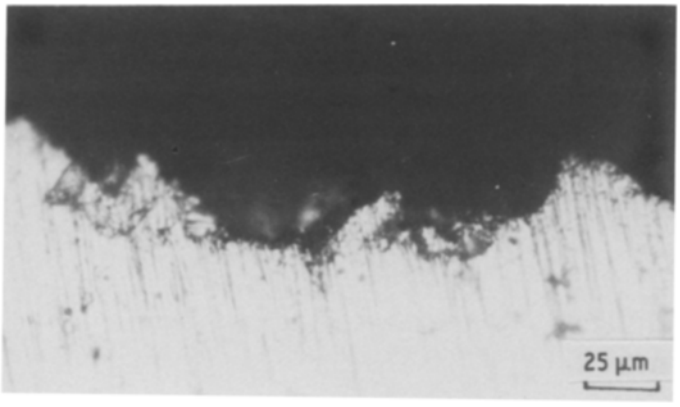

Figure 6 Micrograph showing a cross-section of the corroded surface of Fe–8.25 Al–29.95 Mn–0.85 C age-treated in 6 wt % $FeCl_3$ for 3 days at 25° C.

TABLE II Corrosion rates of various Fe–Al–Mn alloys in 6 wt % $FeCl_3$ solution at 25° C

Alloy	Corrosion rate (mm per year)
316 SS	8
Alloy A	138
Alloy B	121
Alloy C	105

4. Conclusions

The electrochemical polarization curves for the austenitic Fe–8.25 Al–29.95 Mn–0.85 C and Fe–9.33 Al–25.94 Mn–1.45 C alloys, either solution-annealed and/or age-treated, exhibited an active-to-passive transition behaviour in 3.5% NaCl solution. However, these alloys could not passivate as easily as AISI 316 SS. The passive current density of the latter was about one order of magnitude lower than those of the Fe–Al–Mn alloys.

Pitting corrosion accompanied by a severe general attack occurred for all three Fe–Al–Mn alloys in 6% $FeCl_3$ solution. The corrosion rates of these alloys were about 15 times higher than that of AISI 316 SS. The corrosion resistances of the Fe–Al–Mn alloys tested in this study were inferior to that of the conventional austenitic stainless steel.

Figure 7 EDS analysis of pit formed on Fe–8.25 Al–29.95 Mn–0.85 C alloy, solution-treated.

Acknowledgements

The authors gratefully acknowledge the support for this work provided by the National Science Council of the Republic of China under Contract No. NSC74-02010-E006-09. Thanks are also due to Dr C. M. Wan, National Tsing Hua University, for providing the alloys.

References

1. D. SCHMATZ, *Trans. ASM* **52** (1960) 898.
2. R. WANG and F. H. BECK, *Met. Progr.* (March 1983) 72.
3. H. ERHART, R. WANG and R. A. RAPP, *Oxid. Met.* **21** (1984) 81.
4. R. WANG, M. J. STRASZHEIM and R. A. RAPP, *ibid.* **21** (1984) 71.
5. P. TOMASZEWICZ and G. R. WALLWORK, *Corrosion* **40** (1984) 152.
6. R. WANG and R. A. RAPP, in Proceedings of 9th International Corrosion Congress, Toronto, June 1984, Vol. 4, p. 545.
7. E. LUNARSKA, Z. SZKLARSKA-SMIALOWSKA and M. JANIK-CZACHOR, *Corrosion* **31** (1975) 231.
8. N. A. STORCHAK and A. G. DRACHINSKAYA, *Phys. Met. Metall.* **44** (1978) 123.

Received 17 September 1986
and accepted 11 February 1987